SPAWAR

Systems Center PACIFIC

A Methodology for Phased Array Radar Threshold Modeling Using the Advanced Propagation Model (APM)

Amalia E. Barrios

SSC Pacific
San Diego, CA 92152-5001

SSC Pacific
San Diego, California 92152-5001

M. K. Yokoyama, CAPT, USN
Commanding Officer

W. R. Bonwit
Executive Director

ADMINISTRATIVE INFORMATION

Released by
John deGrassie, Head
Atmospheric Propagation Branch

Under authority of
Phillip Juarez, Head
55190 Networks Division

.

EXECUTIVE SUMMARY

This report summarizes the methodology developed to improve the radar threshold modeling capability within the Advanced Refractive Effects Prediction System (AREPS). This work is a culmination of a joint U.S.-Netherlands (NL) project of the Coalition Warfare Program (CWP). The objective of the CWP effort is to enhance radar modeling to enable improved situational awareness of the detection capability of phased array radars, as affected by current meteorological and oceanographic (METOC) conditions.

ACRONYMS

AoI   Area of Interest

APM   Advanced Propagation Model

AREPS   Advanced Refractive Effects Prediction System

CWP   Coalition Warfare Program

EREPS   Engineer's Refractive Effects Prediction System

IREPS   Integrated Refractive Effects Prediction System

MoE   Measures of effectiveness

METOC   Meteorology and Oceanography

NL   Netherlands

NWP   Numerical Weather Prediction

PAR   Phased Array Radar

PDF   Probability Density Function

PRI   Pulse Repetition Interval

PoD   Probability of Detection

PRF   Pulse Repetition Frequency

RCS   Radar Cross Section

RF   Radio Frequency

RFPPAS   Radio Frequency Propagation and Performance Assessment Suite

RRE   Radar Range Equation

SCNR   Signal-to-Clutter-Plus-Noise Ratio

SIR   Signal-to-Interference Ratio

SNR   Signal-to-Noise Ratio

UHF   Ultra High Frequency

CONTENTS

Figures

Tables

1. INTRODUCTION

The Advanced Refractive Effects Prediction System (AREPS) is a U.S. Navy tactical decision aid that has been used fleetwide since the late 1990s (Skolnik, 2007). It allows users to visualize radar performance at various distances, directions, and heights from a given location under a given set of meteorological and oceanographic (METOC) conditions (Barrios et al., 2016). Over the years, the development of AREPS focused on characterization and processing of the underlying atmospheric environment and improving the radio-frequency (RF) propagation models used within the application. This effort has resulted in a suite of widely used propagation models within the DoD as well as high fidelity environmental processing algorithms that provide the optimum environmental information to those propagation models (Barrios, Lynch, Gordon, and Williams, 2016).

The post-processing suite of algorithms to determine measures of effectiveness (MoE) for RF system performance were originally implemented using the method outlined by Lamont Blake (1980) within our predecessor applications, the Integrated Refractive Effects Prediction System (IREPS) and the Engineer's Refractive Effects Prediction System (EREPS). This relatively simple post-processing method was naturally incorporated into the AREPS at its inception. While the environmental characterization (pre-processing component) and propagation modeling (engine component) algorithms have been improved and updated over the years, the post-processing component within the AREPS has not, particularly for phased array radars (PAR). The methodology presented in this report is a first step toward improving the post-processing algorithms for PARs within the AREPS.

2. PHASED ARRAY RADAR CONFIGURATION

Modern PARs are very complex, with numerous operational modes that dynamically change from sector to sector. Within each operational mode, the basic underlying parameters, such as vertical and horizontal beamwidth, power, pulse repetition interval (PRI) or pulse repetition frequency (PRF), etc., can also vary from beam to beam. Figure 1 depicts a PAR where the power and/or PRI is modified for short range or long range search modes. It also illustrates the series of "pencil beam" scans that are used to complete an entire volume of the search space where each beam is emitted at a specific elevation angle and azimuth.

The following discussion describes a simplified configuration of a basic PAR using simple pulsed waveforms to illustrate the methodology presented. The intent is not to delve into antenna theory nor the internal signal processing techniques of modern radars but to demonstrate an improved method to model phased array radar operational modes in the context of a more automated RF performance assessment process when using the APM.

In many PAR systems, the various operational modes are defined such that any one mode will emit several beams, or waveforms, with a pre-defined horizontal and vertical beamwidth, pulse width, PRI (or equivalently a PRF) at a specific elevation angle, α, and at a specific azimuth, φ. This simple geometry is shown in Figure 2. There are other parameters that define the particular waveform(s), w, used for a scan mode, but for the current discussion we will focus on the basic parameters that characterize the set of waveforms for any one scan mode that will necessitate more than one execution of the APM.
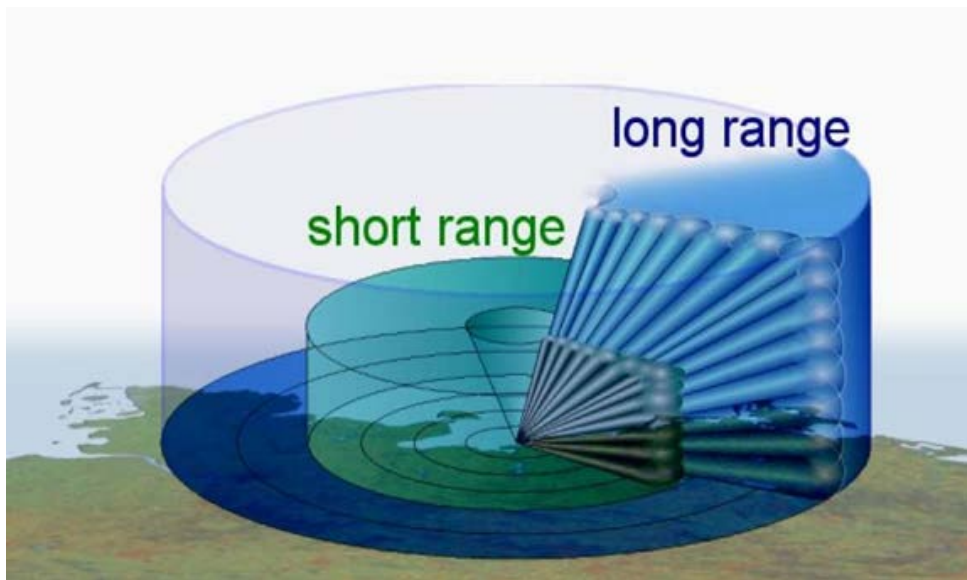
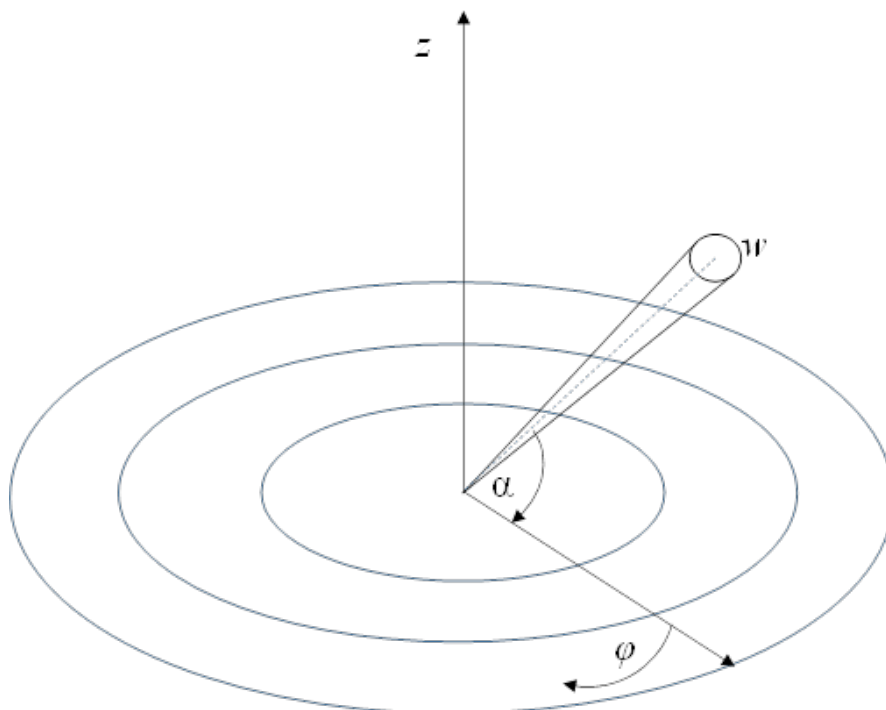Figure 1. PAR short- and long-range scan illustration.

Figure 2. Geometry of emitted waveform, *w*.

In Figure 3, P_t is the peak power, τ is the pulse width, and n_p is the number of pulses. Simply put, the block diagram illustrates that a PAR can operate in various scan modes, and each mode in turn will be characterized by several waveforms with other system parameters describing how and where the waveforms will be emitted. In many cases, only a few waveforms are distinct and various scan modes will use the same waveforms but vary the elevation angle and/or azimuths at which they are emitted, or will alter the power as a function of elevation angle. As shown in Figure 3, all system parameters are labeled as distinct, but in practice many of these parameters can be identical across waveforms and operational scan modes.

Within the AREPS application, the user can specify a set of system parameters where only one waveform is defined to perform a RF prediction. However, as shown in Figure 3, the RF prediction would apply to only a subset of the true functionality of a scan mode of the radar and would not be representative of the radar's capability, particularly if the application assesses a shipboard radar's detection coverage or area of vulnerability.
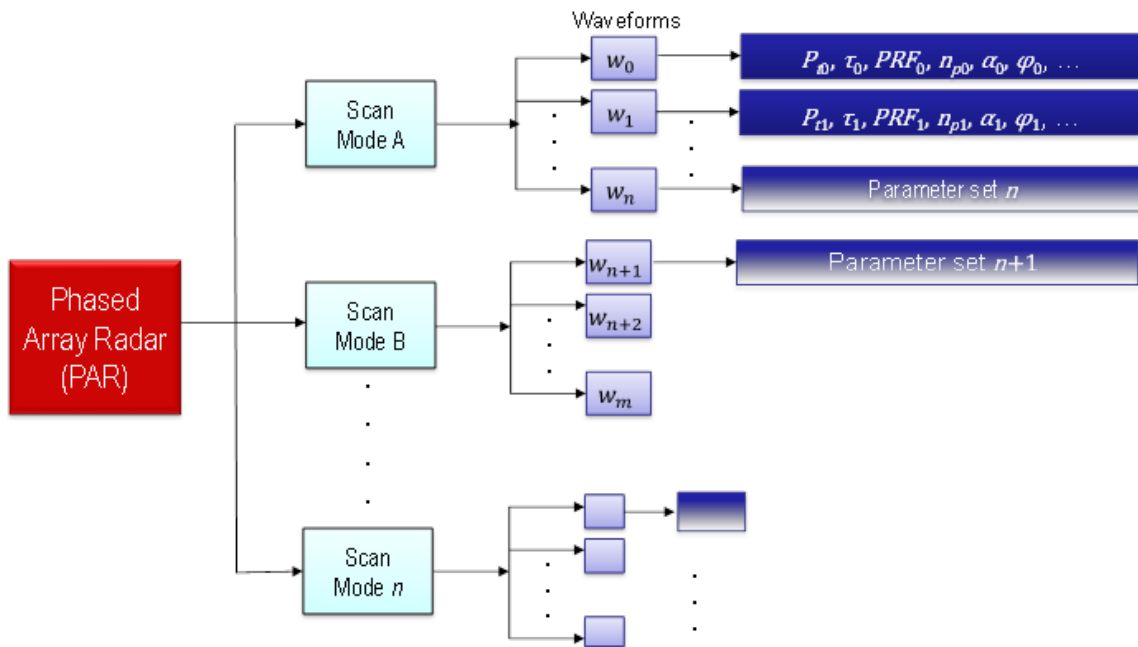
Figure 3. Block diagram of the waveform configuration of a basic PAR.

3. METHODOLOGY

3.1 RF PREDICTION PROCESS

Under the RF Propagation and Performance Assessment Suite (RFPPAS) effort (Barrios et al., 2016), the internal software structure of the APM was completely revamped and updated using modern Fortran language features. It was made thread-safe to take advantage of multi-core systems to efficiently generate RF predictions for large coverage areas or multi-emitter/receiver pairs. It was also modified to generate multiple surface reflectivity arrays corresponding to various pulse widths without the need to re-execute for a given set of remaining inputs. The modifications to the APM were made specifically to better automate the RF prediction process described for a more efficient generation of MoE for PARs.

3

The majority of input parameters required for one execution of the APM primarily pertain to the environment (atmospherics and terrain), with only a handful relating to the actual RF system (Barrios, Lynch, Gordon, and Williams, 2016). The few RF system parameters required are listed in Table 1, along with some general assumptions on typical usage for a general PAR that would dictate a re-execution of the APM.

Table 1. RF system parameter inputs to the APM.

Parameter	Description	Assumptions
f	Frequency	Center transmitting frequency
h_t	Antenna height	Fixed
H, V	Polarization	Fixed (ignoring dual-polarized radars for this discussion)
i_{pat}	Antenna pattern (generic or specific)	Fixed
τ	Pulse width	Variable – waveform dependent
θ_v	Vertical beamwidth	Fixed – can be waveform dependent
θ_h	Horizontal beamwidth	Fixed – can be waveform dependent
α	Elevation (pointing) angle	Variable – waveform dependent

Of course, many PARs will vary certain parameters above that we assume to be fixed, but to simplify the discussion we will use the assumptions as given in Table 1 as these are the most common variations. The overall process can be generalized to include variability in the remaining parameters.

One important parameter that is not an input to the APM but is a critical parameter that would dictate a change in all of the environmental inputs, is the azimuth, φ. For any RF performance assessment application, a change in φ implies a change in the geographic path over which the propagation model is expected to perform. This requires extraction of a new range-dependent refractivity environment from a numerical weather prediction (NWP) forecast as well as extraction of a new terrain profile from a terrain elevation database. Therefore, a change in φ requires a new execution of the APM. The azimuth is also one of the parameters that is assigned to a waveform (or set of waveforms) for an operational scan mode, as described in Section 2.

Let's consider a PAR designed to use several waveforms, w_0, w_1, w_2,…,w_n, where $w_i = w(\tau_i, \text{PRF}_i)$. Next, consider the PAR to operate in several scan modes, S_0, S_1,…,S_n, where S_j uses a subset of waveforms from w_0 to w_n and emits the subset of waveforms at various elevation angles, $\{\alpha_i, i = 1,2,…N\}$, and each S_j in turn operates over a specific set of azimuths, $\{\varphi_k, k = 1,2,…M\}$, for a volumetric scan. If the goal is to efficiently determine the RF performance of a PAR for all modes over a volumetric scan, then all unique pulse widths, elevation angles, and azimuths, over the entire set of S_js must be collected and sorted to minimize the number of execution times of the APM, as illustrated in Figure 4.
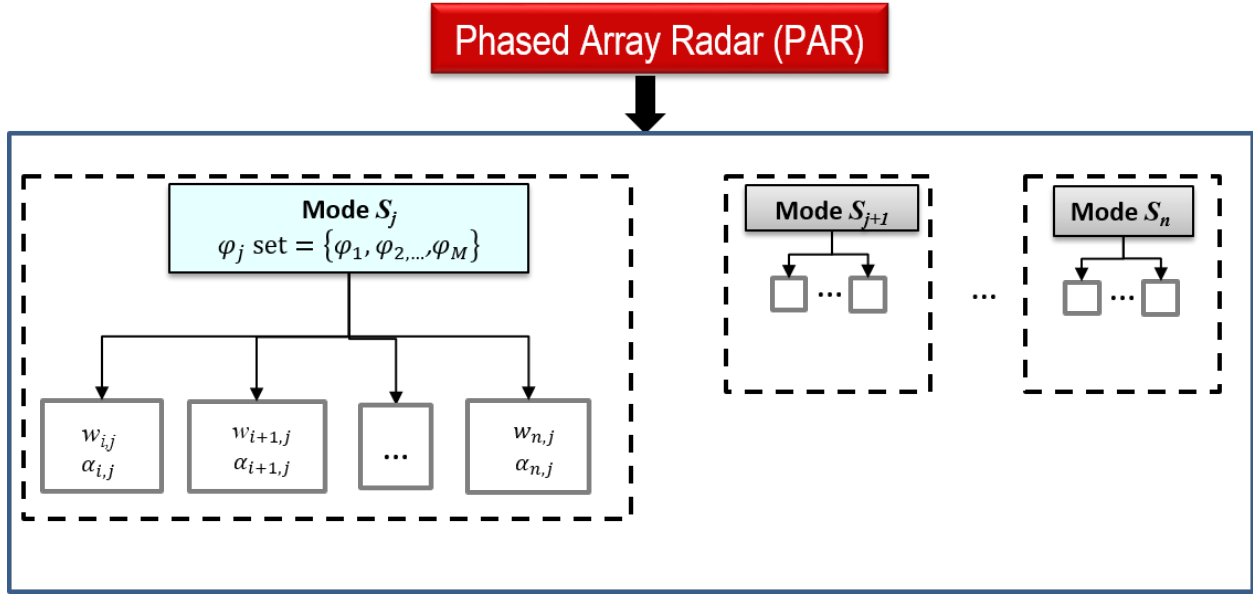
Figure 4. Block diagram of waveform, elevation angle, and azimuth angle assignment for a generic PAR.

In many instances, several waveform parameters are identical across multiple waveforms, and the set of elevation angles and azimuths may change little between scan modes. Although conceptually simple in the determination of the set of parameter values that constitute a new APM execution, the scale of bookkeeping, organization, and manipulation of large volumes of modeled data can be high.

3.2 MEASURES OF EFFECTIVENESS (MoE)

The basic measures of effectiveness for a PAR discussed are detection ranges as a function of probability of detection and the minimum detectable radar cross section (RCS). These are two basic MoE products that provide general detection and counter-detection situational awareness within an area of interest (AOI).

We begin by providing the general power form of the radar range equation (RRE) for computing the received power from a target (Skolnik, 2007):

$$p_r = \frac{p_t g_t g_r \lambda^2 \sigma F^4}{(4\pi)^3 r^4 l_s}$$
(1)

The variables are defined as

p_r = received power (Watts)
p_t = peak transmit power (Watts)
g_t = transmit antenna gain
g_r = receive antenna gain
λ = center (carrier) wavelength (m)
σ = mean RCS of the target (m^2)
F = propagation factor (unitless) determined by the propagation model
r = range to the target (m)
l_s = total transmit and receive system losses.

The propagation factor is a well-known quantity in radiowave propagation literature and is defined as the ratio of electric field strength at a receiver point, including antenna pattern effects but normalized to unity gain antennas, to the electric field that would occur at that point under free space conditions if loss-free isotropic antennas were used for both the transmitter and receiver (Hitney, 1994). This quantity is considered to contain *all* (natural) environmental effects from the propagating medium. However, this is in large part dependent on the particular propagation model being used and the extent of the propagation mechanisms supported by the model. *F* is often overlooked in radar and communications texts and simply "folded" into a catch-all loss quantity where the losses are due to general multi-path and attenuation effects caused by the medium. In this report, *F* is explicitly accounted for and is computed by the APM. The APM is a deterministic, physics-based, radiowave propagation model that can accommodate many environmental effects. However, a detailed discussion of the model will not be provided in this report, but the reader is referred to Barrios (2003) for more detailed background.

In determining the noise power to the radar receiver, the assumption is that all sources of natural noise (cosmic background, solar, etc.) are negligible relative to the internal receiver noise. Obviously, we are concerned primarily with those RF or radar, systems operating at ultra-high frequency (UHF) and higher frequencies. Therefore, we compute the noise power, p_n, from the simple Equation (2).

$$p_n = kT_0 n_f B, \tag{2}$$

where

k = Boltzmann's constant (1.38×10^{-23} watt-sec/K)
T_0 = standard temperature (290 K)
n_f = noise figure of the receiver[1]
B = receiver bandwidth (Hz).bARRIOS

3.2.1 Signal-to-Noise Ratio (SNR)

For a single pulse, the *SNR* of a radar against a target of mean RCS, σ, Equation (3) is then computed from Equation (1) and Equation (2):

$$SNR \equiv \frac{p_r}{p_n} = \frac{p_t g_t g_r \lambda^2 \sigma F^4}{(4\pi)^3 r^4 l_s k T_0 n_f B}. \tag{3}$$

Typically, many of the quantities in Equation (3) are provided, or specified, in dB. As written, Equation (3) does not explicitly state the angular dependence of the antenna gains g_t and g_r. Specifically,

$$g(\theta, \vartheta) = g_{max} |f(\theta, \vartheta)|^2. \tag{4}$$

---

[1] The conventional notation is *N*, or N_f, where the power form of this quantity is unitless. However, the receiver noise is typically provided in dB, so to keep consistent with other power variables designated by lowercase and later represented in dB form using uppercase, the power form is designated as n_f.

In Equation (4), the quantity g_{max} is a constant and refers to the maximum gain of the antenna at boresight, and $f(\theta, \vartheta)$ is the antenna pattern factor. However, the propagation factor, F, implicitly accounts for the antenna gain pattern by way of including $f(\theta, \vartheta)$ in modeling the source field[2] Therefore, we can simplify Equation (3) by using the maximum gains for the transmit and receive antennas.

We can also take advantage of the fact that the primary quantity computed by APM is the one-way propagation loss, L_{APM}, given as Equation (5),

$$L_{APM} = 20 \log_{10}\left(\frac{4\pi r}{\lambda}\right) - 20 \log_{10} F, \tag{5}$$

in dB. Writing Equation (3) in dB form using Equations (4) and (5), and designating uppercase variables as the dB equivalent of their power form (i.e., $P_t = 10 \log_{10} p_t$) gives

$$SNR = P_r - P_n. \tag{6}$$

$$P_r = -38.55 + P_t + 20 \log_{10} f_{MHz} + 10 \log_{10}(\sigma) + G_t + G_r - L_s - 2L_{APM} \tag{7}$$

$$P_n = -143.98 - 10 \log_{10}(\tau) + N_f. \tag{8}$$

In Equation (7), constants and conversion factors used to convert λ to frequency in MHz, f_{MHz}, results in the first term constant. P_t is in dBW, and the maximum antenna gains (G_t, G_r) are in dBi. In Equation (8), the noise figure, N_f, is in dB, the pulse width for an optimum receiver bandwidth $\left(B = \frac{1}{\tau}\right)$ is used, and constants and conversion factors are combined to obtain the first term constant, where the pulse width is in µs.

Ultimately, it is the SNR that is the determining factor in how a radar performs. Of course, most radars determine whether a target is present based on multiple pulses, not just one. To determine if a PAR can detect a target, the SNR must exceed some minimum detectable signal threshold, SNR_{min}. For a PAR using coherent processing (amplitude and phase of return pulses), Equation (3) can be modified by including the number of pulses, n_p, in the numerator (and modifying Equation (7) accordingly). This numerator represents the improved signal processing gain by coherently integrating n_p pulses. For a PAR using non-coherent processing (amplitude only), the relationship is not as simple (Richards, Scheer, and Holm, 2010). Also, as defined in Equation (7), σ represents the mean RCS of the target. The RCS of a target, in reality, will fluctuate due to many facets and shapes comprising the target surface. Therefore, even if using coherent processing, determining the SNR using Equation (7) by applying a gain from n_p pulses may not be entirely valid for a realistic [fluctuating] target. However we can alleviate these complications if we determine the equivalent single-sample SNR_{min} for a given probability of detection, P_d, probability of false alarm, P_{fa}, number of pulses integrated, and the particular target fluctuation model used. This is done using Shnidman's equations (Shnidman, 2002), described in Section 3.2.3. First, a brief description of the fluctuating models employed in this methodology will be discussed.

---

[2] Some texts explicitly refer to F as the *pattern* propagation factor to emphasize its angular dependence (i.e., $F(\theta, \vartheta)$).

3.2.2 Fluctuation Models

In the method presented in this report, we look at the four statistical fluctuation models developed by Swerling (Richards, Scheer, and Holm, 2010). The four models are composed of two probability density functions (PDF), Rayleigh and 4th degree chi-square, with two fluctuation rates. These are referred to as Swerling cases 1, 2, 3, and 4 and are listed in Table 2. The fluctuation rates correspond to the decorrelation properties for each PDF.

The non-fluctuation, or steady, target model is referred to as Swerling case 0 or Swerling case 5 in the literature. Swerling cases 1 through 4 are of primary interest and are used in determining SNR_{min}.

Table 2. Swerling models.

PDF	Swerling Case	Decorrelation	Description
Rayleigh (exponential)	1	dwell-to-dwell	Target has many scatterers, none are dominant. Set of N returned pulses are correlated within a dwell but independent with the next set of N pulses on the next dwell.
Rayleigh (exponential)	2	pulse-to-pulse	Target has many scatterers, none are dominant. Set of N returned pulses are independent from each other within a dwell.
4th degree chi-square	3	dwell-to-dwell	Target has many scatterers, with one dominant. Set of N returned pulses are correlated within a dwell but independent with the next set of N pulses on the next dwell.
4th degree chi-square	4	pulse-to-pulse	Target has many scatterers, with one dominant. Set of N returned pulses are independent from each other within a dwell.

The question now becomes, which Swerling case should be used for a given target? Regardless, if a complete measurement set of RCS values as a function of elevation and the azimuth angle was available to determine a more appropriate Swerling case, the orientation and aspect angle of the target to the antenna boresight is unknown in practice. Also, the RCS values as a function of angle for any target are typically unavailable.

Therefore, a reasonable option is to apply all Swerling cases, which implies that both PDFs are employed in determining SNR_{min}. For specific capabilities of a PAR, such as one that uses frequency agility, this inherently forces decorrelation from pulse-to-pulse, so only Swerling cases 2 and 4 need be applied (Richards, Scheer, and Holm, 2010). Determining multiple SNR_{min} values also allows the radar performance to be described by lower and upper bounds of the particular metric (i.e., detection range) due to various unknowns of the target.

3.2.3 Shnidman's Equations

There are exact equations to determine a P_d given SNR, but the inverse cannot be expressed analytically (Shnidman, 2002). However, Shnidman developed a set of empirical approximations that allow the computation of a single-sample SNR required (i.e., SNR_{min}) to obtain a given P_d, P_{fa}, N, and Swerling case when multiple pulses are non-coherently integrated. Shnidman's equations are also valid over a wide range of parameters with less than 1 dB of error in the range $0.1 \leq P_d \leq 0.99, 1 \leq N \leq 100$, and $10^{-9} \leq P_{fa} \leq 10^{-3}$, where over most of this range errors are less than 0.5 dB. Slightly larger errors occur at the extreme range of P_{fa}. Shnidman also provides an extension set of equations that result in less error, applicable for $0.99 \leq P_d \leq 0.9992$ and $1 \leq N \leq 20$; however, for our application, this particular range of P_d is not considered.

The single sample SNR_{min} is determined by the set of equations defined below, N being the number of samples integrated.

$$SNR_0 = \eta \left[\eta + 2\sqrt{\frac{N}{2} + \left(a - \frac{1}{4}\right)} \right], \tag{9}$$

where

$a = 0$ for $N < 40$
$a = \frac{1}{4}$ for $N \geq 40$.

$$\eta = \sqrt{-0.8 \ln\left[4P_{fa}(1 - P_{fa})\right]} + sign(P_d - 0.5)\sqrt{-0.8 \ln\left[4P_d(1 - P_d)\right]}, \tag{10}$$

SNR_0 represents the value, in power form, for the non-fluctuating case (Swerling case 0). We apply the various Swerling cases using values of the fluctuation parameter, K, according to Table 3.

Table 3. K value for each Swerling case.

Swerling Case	K
1	1
2	N
3	2
4	2N

The K values in Table 3 are then used to compute quantities C_1 and C_2:

$$C_1 = \frac{1}{K}\left([(17.7006P_d - 18.4496)P_d + 14.5339]P_d - 3.525\right) \tag{11}$$

$$C_2 = \frac{1}{K}\left(e^{(27.31P_d - 25.14)} + (P_d - 0.8)\left[0.7 \ln\left(\frac{10^{-5}}{P_{fa}}\right) + \frac{(2N-20)}{80}\right]\right). \tag{12}$$

A correction term in dB is then computed from C_1 and C_2:

$$C_{dB} = C_1; \text{ for } 0.1 \leq P_d \leq 0.87 \tag{13}$$

$$C_{dB} = C_1 + C_2; \text{ for } 0.87 \leq P_d \leq 0.99. \tag{14}$$

The equivalent single sample SNR_{min} required to non-coherently integrate N pulses is then computed as

$$C = 10^{\left(C_{dB}/10\right)}$$

$$SNR_{min} = 10 \log_{10}\left(\frac{C*SNR_0}{N}\right). \tag{15}$$

As mentioned in Section 3.2.1, we can compute the total SNR for n_p pulses for the coherent processing case, or, as done for the non-coherent case, simply compute the equivalent single sample SNR_{min} for the appropriate Swerling cases. From Curry (2005): "Detection using a single pulse and detection using a series of pulses coherently integrated are treated together here, because in both cases the signal is a single sample of the target amplitude distribution. A burst of coherently integrated pulses generates a single target observation, and produces the same target statistics as a single pulse." Since a coherent dwell is n_p times the number of pulses coherently integrated, this implies Swerling cases 1 and 3 for the fluctuation target models[3]. The required SNR is then determined from $SNR_{min} = SNR_1 - 10 \log_{10}(n_p)$, where SNR_1 is the required SNR for a single pulse.

3.2.4 Signal-to-Clutter-Plus-Noise Ratio (SCNR)

Once SNR_{min} is computed, the PAR performance is assessed by comparing SNR_{min} with the predicted SNR using Equation (6) through Equation (8), taking into account all effects from the medium. However, this does not represent a fair assessment because the radar's detection performance is based on the processed signal exceeding all sources of noise and interference. Therefore, the signal-to-interference ratio (SIR) must be computed to truly assess performance:

$$SIR \equiv \frac{S}{C+N+J} = \frac{p_r}{p_c+p_n+p_j}, \tag{16}$$

where p_c is the returned clutter power, p_j is the power due to jamming, and p_r and p_n are as previously defined. In reality, not all three terms in the denominator are equally dominant. We consider system noise and surface clutter to be ubiquitous, whereas interference due to jammers are considered for specific applications. Therefore, to simplify the method presented, we consider only the interference from clutter and noise, or the SCNR.

---

[3] Note that for $N = 1$, SNR_{min} values for Swerling cases 1 and 2 are identical and that for Swerling cases 3 and 4 are identical for a given P_d and P_{fa}.

First, the clutter power, p_c, can be computed by modifying the RRE:

$$p_c = \frac{p_t g_t g_r \lambda^2 \sigma_c F_c^4}{(4\pi)^3 r^4 l_s}. \tag{17}$$

Notice that all terms, with the exception of σ_c and F_c, are defined as in Equation (1). The "target" in this case is the surface, and σ_c represents the surface clutter cross section. F_c is the near-surface propagation factor[4]. In dB form, Equation (17) becomes

$$P_c = 16.57 + P_t + \sigma_{c(dB)} + G_t + G_r - 20 \log_{10} f_{MHz} - 40 \log_{10}(r) - L_{sys} + 2F_{c(dB)}. \tag{18}$$

Again, the first term constant comes from the constant in the denominator of equation (17) and conversion factors to couch Equation (18) in terms of f_{MHz} vice λ in meters. Both quantities $\sigma_{c(dB)}$ and $F_{c(dB)}$ are specifically returned from the APM, where $\sigma_{c(dB)} = 10 \log_{10}(\sigma_c)$ and $F_{c(dB)} = 20 \log_{10}(F_c)$.

Using Equation (7), Equation (8), and Equation (18), we compute P_r, P_n, and P_c, respectively (more tractable in dB form). Converting P_c and P_n to their power forms we can then compute the SCNR using

$$SCNR = P_r - P_{cn}, \tag{19}$$

where

$$P_{cn} = 10 \log_{10}(p_c + p_n). \tag{20}$$

It is the final quantity, $SCNR$, defined by Equations (19) and (20), which is compared with SNR_{min} to assess a radar's performance.

3.2.5 Minimum Detectable RCS

It naturally follows that the minimum detectable RCS in dB, $\sigma_{min(dB)}$, is that which is derived from the minimum SNR required for detection, SNR_{min} (Barrios et al., 2016). Using Equations (7), (19), and (20), we can write $\sigma_{min(dB)}$ as

$$\sigma_{min(dB)} = 38.55 + SNR_{min} + P_{cn} + L_{sys} - P_t - 20 \log_{10} f_{MHz} - G_t - G_r + 2L_{APM}. \tag{21}$$

3.3 PROCESS FLOW

One additional parameter that is associated with a waveform used for a particular scan mode is the dwell time, t_d. The waveform is then described by the parameters, τ, PRF (or PRI), and t_d: $w_i = \{ \tau_i, PRF_i, t_{di} \}$.

---

[4] To be technically correct, this should be the incident propagation factor; however, what is computed from the APM and returned is the near-surface propagation factor, which is designated as F_c.

The number of pulses is determined by Richards, Scheer, and Holm (2010):

$$n_p = t_d PRF = \frac{t_d}{PRI}. \tag{22}$$

The process flow is now described as follows.

1. All waveforms for applicable scan modes are collected and each set of unique azimuth, elevation angle, and pulse width triplet, $\{\varphi_i, \alpha_i, \tau_i\}$, are determined and sorted.
2. Propagation loss is then determined from the APM for each triplet. Propagation loss is computed in the form of a vertical coverage (vertical 2-dimensional plane) for each azimuth where loss is determined as a function of range and height.
3. All vertical coverage loss arrays and their associated waveforms are then organized according to their respective scan modes. For each vertical coverage of propagation loss, the SCNR is computed based on the set of equations defined in Sections 3.2.1 and 3.2.4. Each $SCNR_i$ now represents the SCNR corresponding to a particular waveform and dwell time for a given scan mode.
4. For a given value of P_{fa} and P_d, SNR_{min} is computed for each n_p associated with each waveform for all applicable Swerling cases (i.e., $SNR_{min}(n_p,K)$).
5. All receiver geometries (range and heights) where $SCNR_i$ is greater than $SNR_{min}(n_p,K)$, then represents the P_d probability of detection (PoD_i) corresponding to the given P_{fa} and Swerling case for the given scan mode.
6. The composite PoD is then determined from the maximum of all vertical coverage grids of PoD_i associated with each w_i applied at each azimuth and scan mode:

$$PoD_{max} = \max_i(PoD_i). \tag{23}$$

4. EXAMPLE – COHERENT PROCESSING

This process flow is best illustrated by an example where all parameters have been selected to demonstrate the methodology and bear no resemblance to any real radar.

We consider the simple case of an S-Band radar using coherent integration. System parameters for the radar are listed in Table 4, and the radar is configured to use six waveforms with the parameters shown in Table 5. Now consider two operational scan modes, Mode 1 and Mode 2 (item #11 in Table 4), where each mode is described by the combination of waveform, dwell time, and elevation angles listed in Table 6. Note that we are only considering low elevation angles, where anomalous propagation effects are most pronounced. Also, for the sake of simplicity, the assumption in this report is that each mode is assigned to operate at every 1° azimuth from 0° to 359°.

Table 4. Example radar parameters.

Item	Description	Value
1	Tx antenna height	50 ft AGL
2	Frequency	3000 MHz
3	Peak power	100 kW
4	Receiver noise figure	0 dB
5	Total (Tx+Rx) system loss	6 dB
6	Antenna pattern	SINC(x)
7	Polarization	Vertical
8	Tx/Rx antenna gain	35 dBi
9	Vertical beamwidth	1.5°
10	Horizontal beamwidth	1.5°
11	Scan modes	1 and 2
12	Target RCS	10 dBsm (10 m^2)
13	Integration processor	Coherent
14	Swerling cases	1, 3
15	Probability of false alarm	1e-8

Table 5. Waveform parameters.

Waveform	τ (μsec)	PRI (μsec)	PRF (Hz)
w_1	51.0	2200	454
w_2	25.0	1400	714
w_3	12.0	800	1250
w_4	25.0	1900	526
w_5	12.0	1000	1000
w_6	6.0	750	1333

Table 6. Scan mode parameters.

Mode 1				Mode 2			
Waveform	α (deg)	t_d (msec)	n_p	Waveform	α (deg)	t_d (msec)	n_p
w_1	0.0	20	9	w_2	0.25	30	21
w_1	0.75	15	7	w_4	0.75	25	13
w_2	1.5	10	7	w_3	1.5	9	11
w_4	2.25	10	5	w_5	2.25	9	9
w_3	3.0	5	6	w_6	3.0	7	9
w_3	4.0	4	5	w_6	5.0	5	6

In completing steps 1 and 2 of Section 3.3, we sort all elevation angles and pulse widths and combine those used for both modes to minimize the APM execution. Notice that the respective waveforms for each mode are applied at six distinct elevation angles. However, four of these elevation angles (0.75°, 1.5°, 2.25°, and 3.0°) are common between each mode. Therefore, to determine the overall radar performance at any azimuth for both modes simultaneously, only eight executions of the APM are required instead of twelve. For those elevation angles that are common, the propagation loss will be identical for both modes[5], but not P_c, or specifically, the quantities determined from the APM, $\sigma_{c(dB)}$ and $F_{c(dB)}$, as these will be a function of the pulse width, τ (or the corresponding w). The APM now has the ability to generate multiple $\sigma_{c(dB)}$ and $F_{c(dB)}$ values for multiple τs with its recent modernization (Barrios et al, 2016), without the need for multiple computations of the vertical plane propagation loss. This capability will only slightly increase execution time, as the majority of the run time is due to the computation of vertical coverage propagation loss. However, the ability to re-use propagation loss computed for the same azimuth for multiple waveforms improves the overall efficiency in determining radar performance for all operational scan modes simultaneously. Propagation loss for the six elevation angles used for Mode 1 are shown in Figure 5. For this example, the environment is a homogeneous surface-based duct over sea water with a 10 m/s wind speed.
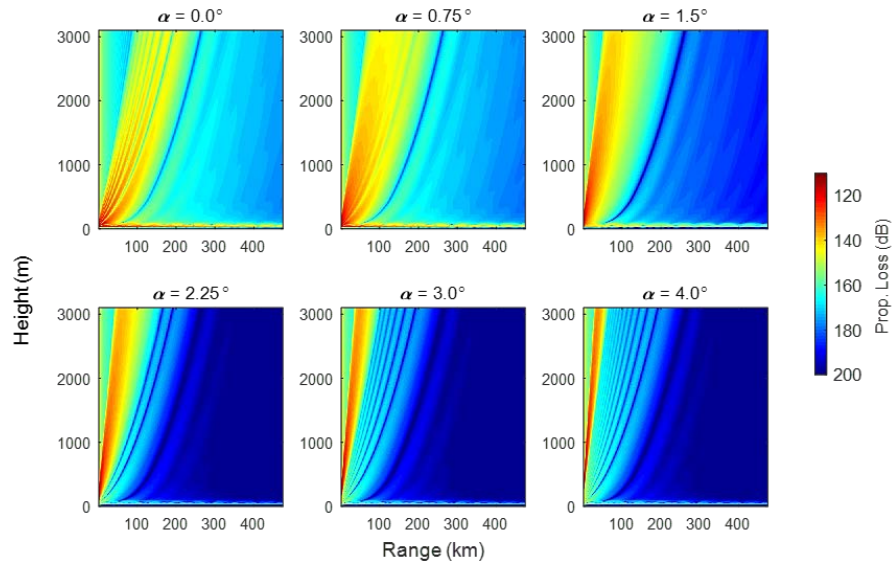

Figure 5. Propagation loss for elevation angles (or associated waveforms) from Mode 1.

---

[5] Of course, this is not true if both modes operate over distinct azimuths. In practice there will be some common azimuths, which will add to the complexity of the bookkeeping involved (i.e., one mode may operate at every 1° while another mode may operate at every 1.5°).

Following step 3, we now determine the SCNR for all corresponding APM runs for each mode. Again, showing only those SCNR vertical coverage diagrams for Mode 1, we see the effects of clutter in Figure 6.
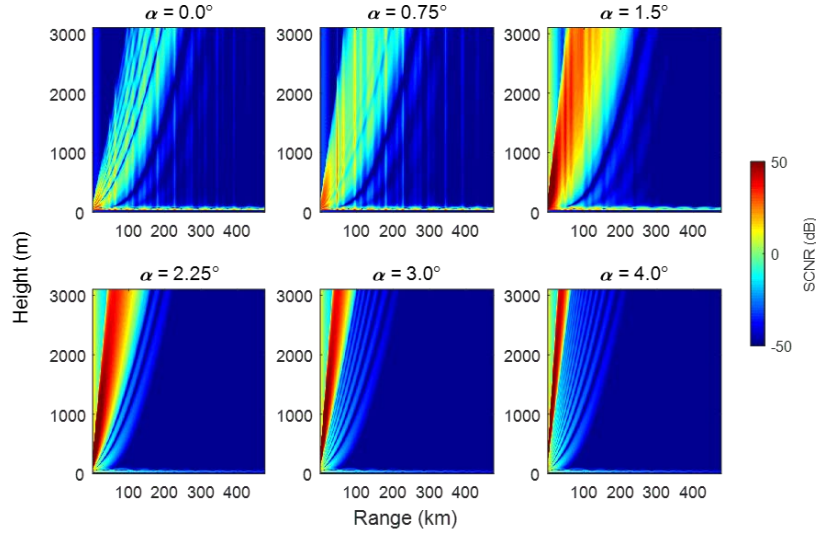

Figure 6. SCNR for waveforms and elevation angles corresponding to Mode 1.

From step 4 and the discussion in Section 3.2.3, we know that the appropriate Swerling cases to apply for a fluctuating target in combination with a PAR that uses coherent integration are Swerling cases 1 and 3. The equivalent single-sample minimum required SNR, adjusted by the n_p value associated with each waveform and dwell time, is now computed for all P_d values of interest. In this example, we consider P_d values of 0.1, 0.2, etc., to 0.9, with the P_{fa} value in Table 4 (item #15). Following step 5, the PoD at any receiver point is that value where the SCNR is greater than $SNR_{min}(P_d, P_{fa}, n_p, K)$ for each Swerling case. The vertical coverage of PoD is shown in Figure 7 for each waveform, elevation angle, and dwell time combination for Mode 1 and Swerling case 1. There is a corresponding set of six PoD coverage arrays for Swerling case 3 (not shown).
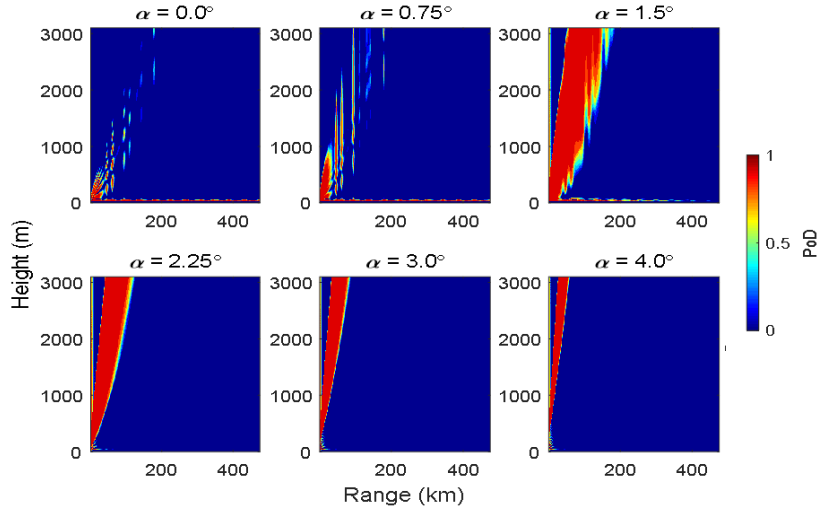
Figure 7. PoD for waveforms and elevation angles for
Mode 1, Swerling Case 1.

Finally, from step 6 we get the composite PoD for the azimuth for each Swerling case. The PoD coverages for Mode 1 are shown in Figure 8. Of course, in computing the propagation loss and SCNR for Mode 1, we are able to re-use four of the six propagation loss arrays in determining the PoD coverage for Mode 2. For these cases, $\sigma_{c(dB)}$ and $F_{c(dB)}$ were computed simultaneously for both Mode 1 and 2 waveforms. Therefore, in determining the PoD coverages for Mode 2, only two additional APM executions are needed. The SCNR coverages for all Mode 2 waveforms are computed as we did for Mode 1 with the final Mode 2 PoD coverages for both Swerling cases shown in Figure 9.
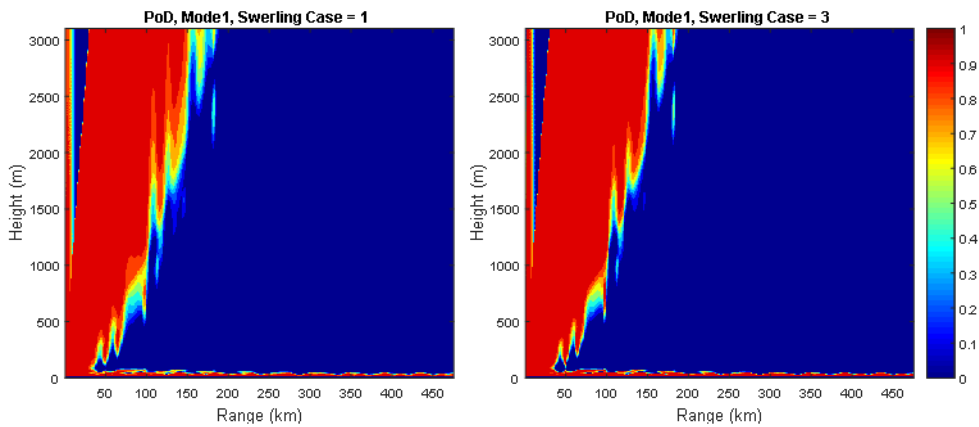
Figure 8. Mode 1 PoD coverage for Swerling cases 1 (left) and 3 (right).
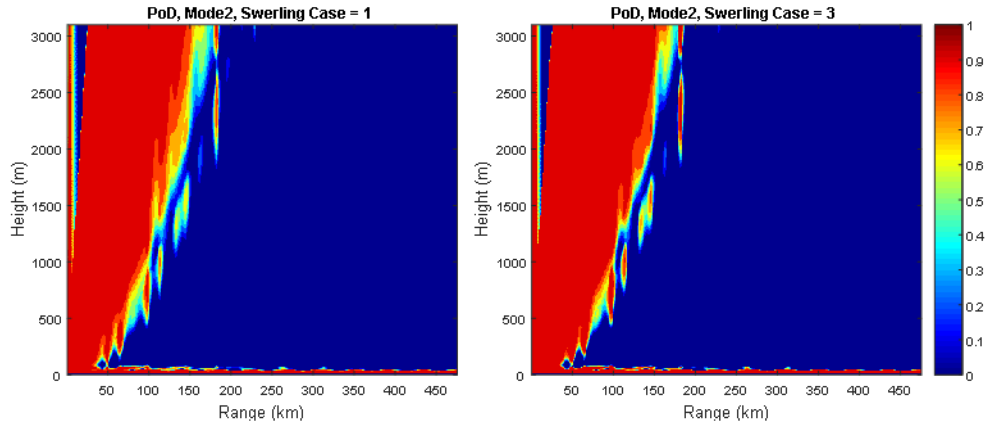
Figure 9. Mode 2 PoD coverage for Swerling cases 1 (left) and 3 (right).

At first glance, there appears to be little difference between the PoD coverage using one fluctuation model over another for a given scan mode. However, detection range is typically ascertained, or reviewed, at specific target heights. Extracting the detection range at select heights for both Swerling cases, we see there is indeed some differences depending on which fluctuation model is used. Figure 10 shows the 90% PoD detection ranges for Mode 1, at near-surface and higher altitudes, for a target with RCS of 10 dBsm (item #12 in Table 4). Detection ranges for Swerling case 1 are shown in thick blue lines while those for Swerling case 3 are overlayed in thin red lines. At almost all target heights shown, the detection ranges vary, sometimes substantially. For instance, at a target height of 1000 m the detection range using Swerling case 1 is roughly 75 km (40.5 nm) whereas that shown for Swerling case 3 is almost 100 km (54 nm)—a difference of 25 km (13.5 nm). Similarly, for the lowest altitude shown, there are ranges between 300–325 km that are predicted using Swerling case 3 but none within that range for Swerling case 1..
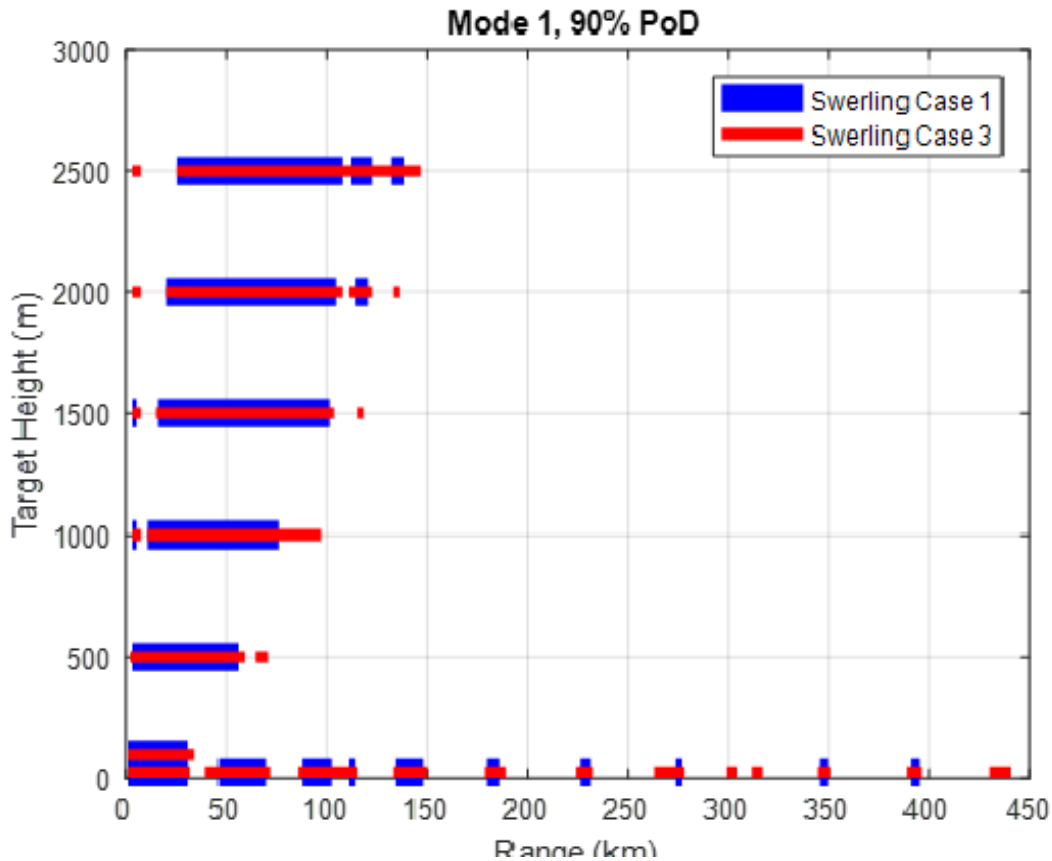
Figure 10. Detection ranges (90% PoD) for Mode 1 against a 10 dBsm target.

When viewed in terms of bounding the estimated detection range based on unknowns of the target, we can use the results from applying both fluctuation models to present the predicted detection range as shown in Figure 11. Results for both scan modes 1 and 2 are shown. In Figure 11, the detection ranges predicted using both fluctuation models (Swerling cases 1 and 3) are shown in red and are labeled as high to indicate there is "high" confidence for these predictions (in a qualitative sense) while those detection ranges predicted by only one of the fluctuation models (Swerling case 3) are labeled as "low" confidence. This way one can view the above representation from both detection and counter-detection perspectives. For instance, one can instantly view the "high" detection ranges as a conservative estimate when determining ownship areas of defensibility/vulnerability – regardless of imprecise knowledge of the target. Those extended detection ranges (ranges indicated by red plus green) can be interpreted as conservative estimates for ownship detection by a threat emitter.
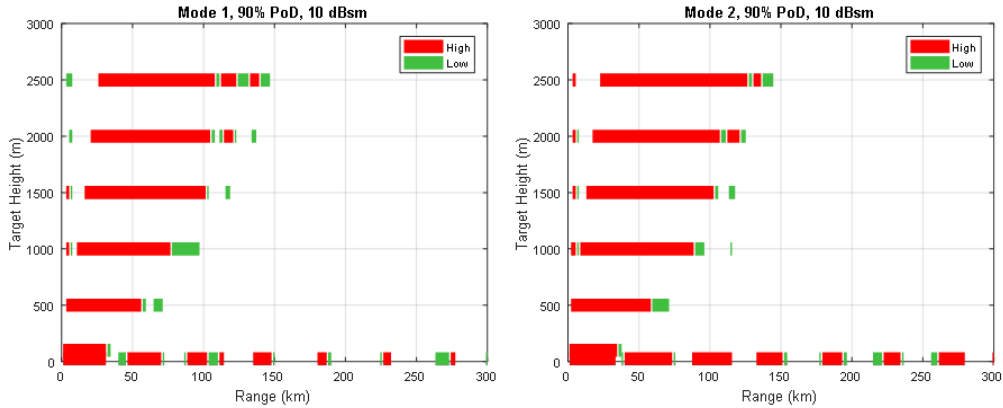
Figure 11. 90% PoD detection range for Modes 1 (left) and 2 (right). Colors indicate high confidence (red) and low confidence (green).

To estimate radar performance over an area of interest (AoI), we now apply the same concept to display area coverage for a specific PoD at a given height, where the refractive environment is a range-, height-, and azimuth-varying environment produced by a numerical weather prediction (NWP) model. This is shown in Figure 12 where 90% PoD detection coverage is displayed simultaneously for both scan modes with parameters from Table 4 to Table 6. An NWP-driven environment is typically what is used in operation, and this example contains highly variable anomalous propagation conditions as seen by the high-detection "range rings" produced. The Mode 1 90% PoD detection coverage for a 10-dBsm target at 6.0 m (19.7 ft) is shown on the left and that for Mode 2 is shown on the right. Similar to Figure 11, the green and red colors indicate high and low confidence of detection range within each mode. The dashed ovals also highlight where one scan mode may provide better coverage over a particular sector.

To compute the information necessary to produce the left graphic in Figure 12 requires 2160 APM executions (six unique waveform/elevation angle combinations per azimuth, multiplied by 360 azimuths). A simple algorithm of replicating this for another scan mode would require twice the number of executions – for our example, 4320. However, the methodology presented in this report, where APM results are re-used and applied to another scan mode, requires only 2880 in total to produce the information necessary for both scan modes (for Mode 2, only two APM runs per azimuth are needed, resulting in an additional 720 APM executions).
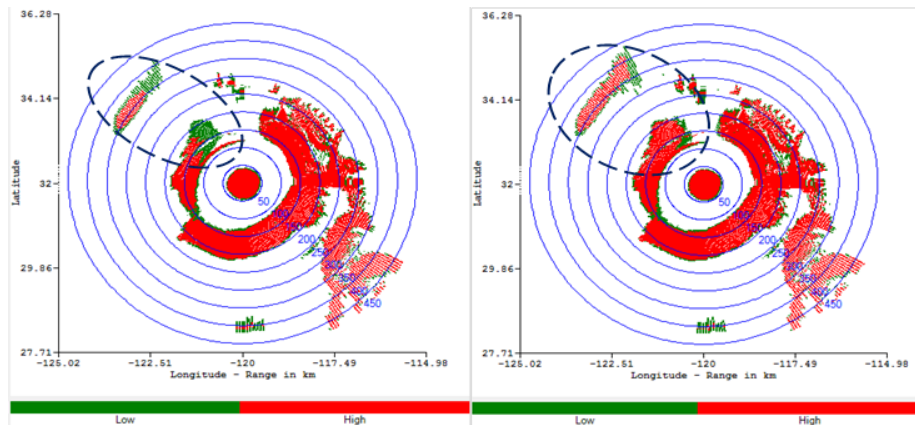

Figure 12. 90% PoD area coverage for Mode 1 (left) and Mode 2 (right) at a target height of 6 m (19.7 ft).

19

5. EXAMPLE – NON-COHERENT PROCESSING

For the non-coherent processor, this is simply an extension of the coherent processing example discussed previously. For the same RF parameters, waveforms, and dwell times, but altering item 13 inTable 4 to a non-coherent processor, the number of APM executions required are identical. The only difference are the number of fluctuation models applied to determine the range of SNR_{min}s needed to obtain the final MoE metric. In this case, all four fluctuation models (Swerling cases 1–4) are used, along with our pre-set values for P_d, P_{fa}, and n_p in Equations 9–15 to obtain four detection ranges for a given P_d. In keeping with a 'green/yellow/red' figure of merit, the equivalent detection coverage for a PAR using non-coherent integration is shown Figure 13. In this example, areas where the SCNR exceeded all four SNR_{min}s in step 5 ($SNR_{min}(n_p,K)$ for each n_p and K combination associated with all four Swerling cases and dwell times) are indicated by areas in red (high). Those exceeding only three SNR_{min}s are indicated in yellow (medium) and those areas where the SCNR exceeded just two SNR_{min}s are indicated in green (low). Of course, the threshold metric can be adjusted depending on the user's particular application (i.e., areas where the SCNR exceeded two, instead of three, SNR_{min}s may be considered 'medium' confidence).
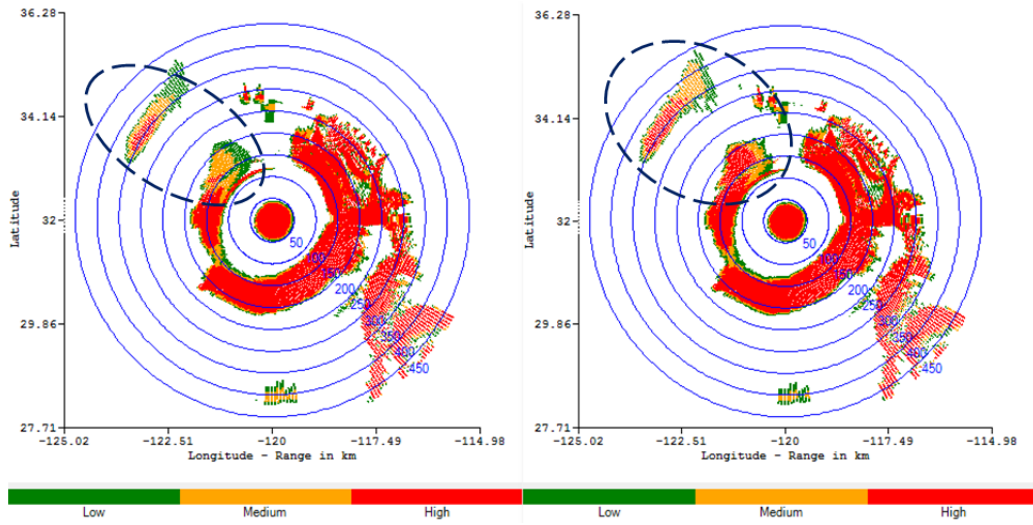

Figure 13. 90% PoD area coverage for Mode 1 (left) and Mode 2 (right) at target area heght of 6 m (19.7 ft) for a non-coherent PAR..

6. EXAMPLE – MINIMUM DETECTABLE RCS

To get an equivalent performance metric for σ_{min} is much the same procedure as outlined in Section 3.3. However, in this case we use Equation (21) to determine σ_{min} for each waveform and elevation angle combination for a given P_d and Swerling case, i_{sw}. Then the composite σ_{min} for each Swerling case is determined by taking the minimum of all vertical σ_{min} grids:

$$\sigma_{min}(i_{sw}) = \min_k\left[\sigma_{min_k}(i_{sw})\right]. \tag{24}$$

20

Figure 14 shows the composite σ_{min} for both Swerling cases 1 and 3 with a 90% PoD for the coherent processor example illustrated in Section 4. In this case, the difference between both results is a constant, $\Delta\sigma_{min}$, represented by the difference in the minimum of all SNR_{min}s computed for each Swerling case,

$$\Delta\sigma_{min} = |\sigma_{min}(i_{sw} = 1) - \sigma_{min}(i_{sw} = 3)|$$

$$= \left| \min_k SNR_{min}\left(w_k, \alpha_k, n_{p_k}\right)\Big|_{i_{sw}=1} - \min_k SNR_{min}\left(w_k, \alpha_k, n_{p_k}\right)\Big|_{i_{sw}=3} \right|.$$

Therefore, a final representation of the minimum detectable RCS over all applicable Swerling cases for a given P_d and P_{fa}, may be displayed as the minimum [of all applicable Swerling cases] conditioned that σ_{min} at any receiver point may have a value between σ_{min} and $\sigma_{min} + \Delta\sigma_{min}$.
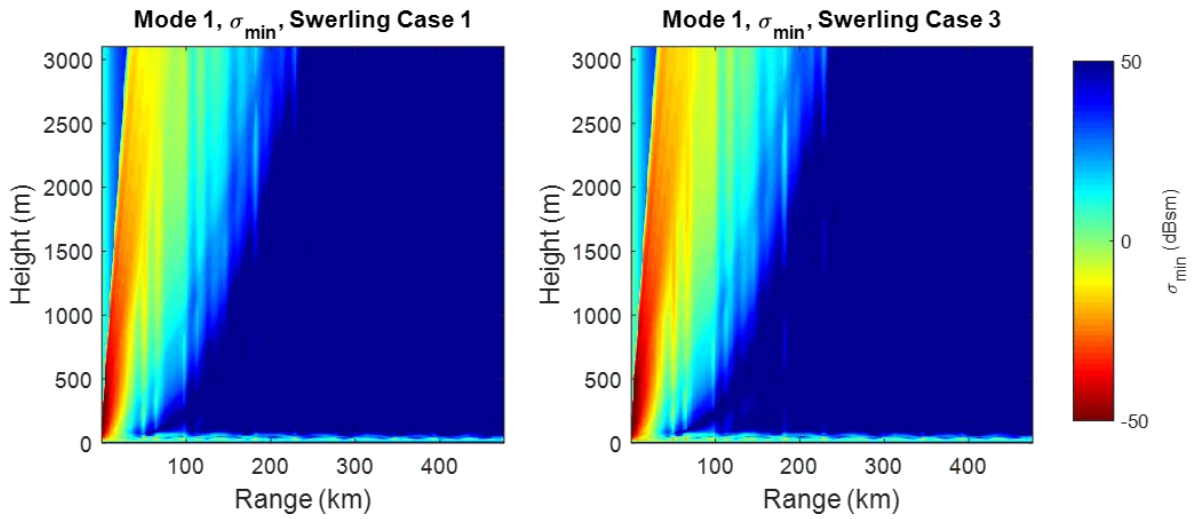

Figure 14. Minimum detectable RCS for 90% PoD, Mode 1, Swerling cases 1 (left) and 3 (right).

7. SUMMARY

A methodology to improve radar performance prediction for a PAR is presented in this report. This method maximizes re-use of propagation modeling results from the APM and incorporates multiple waveforms and scan parameters from a PAR. While the examples discussed are simple, the method presented is meant to establish a fundamental baseline upon which more sophisticated waveforms and operational scan modes can be applied. One of the obstacles in realizing this scheme is obtaining much of the information regarding a PAR's configuration. However, the methodology discussed in this report is a greatly improved algorithm that increases the overall efficiency of determining a PAR's radar performance when compared to current algorithms employed within the AREPS.

REFERENCES

Barrios, A. E., S. D. Lynch, N. Gordon, and E. Williams. 2016. "Radio Frequency Propagation and Performance Assessment Suite (RFPPAS)." Technical Report 3043 (September). Space and Naval Warfare Systems Center Pacific, San Diego, CA.

Barrios, A., T. Rogers, R. Navarro, E. Williams, K. Horgan, V. Wiss, S. Billingsley, R. Marshall, V. van Leijen, T. Wilbrink, F. Bolderheij, and J. Derksen. 2016. "Radio Frequency Performance Prediction in the North Sea." Technical Report 3028 (September). Space and Naval Warfare Systems Center Pacific, San Diego, CA.

Barrios, A. 2003. "Considerations in the Development of the Advanced Propagation Model (APM) For U.S. Navy Applications." *Proceedings of the International Radar Conference* (pp. 77–82). September 3–5, Adelaide, Australia.

Blake, L.V. 1980. *Radar Range Performance Analysis*. D.C. Heath and Company, Lexington, MA.

Curry, G. R. 2005. *Radar System Performance Modeling*. 2nd ed. Artech House, Norwood, MA.

Hitney, H. V. 1994. "Refractive Effects from VHF to EHF: Propagation Mechanisms," *Propagation Modelling and Decision Aids for Communications, Radar and Navigation Systems*, pp. 4A-4B, NATO AGARD Lecture Series 196, Ottawa, Canada.

Richards, M. A., J. A. Scheer, and W. A. Holm. 2010. *Principles of Modern Radar, Vol 1: Basic Principles*. SciTech Publishing, Inc., Raleigh, NC.

Shnidman, D. A. 2002. "Determination of Required SNR Values," *IEEE Transactions on Aerospace and Electronic Systems* 38(3):1059–1064.

Skolnik, M. 2007. *Radar Handbook*. 3rd ed. The McGraw-Hill Companies, New York, NY.

REPORT DOCUMENTATION PAGE

1. REPORT DATE *(DD-MM-YYYY)*	2. REPORT TYPE	3. DATES COVERED *(From - To)*
October 2017	Final	

4. TITLE AND SUBTITLE	5a. CONTRACT NUMBER
A Methodology for Phased Array Radar Threshold Modeling Using the Advanced Propagation Model (APM)	5b. GRANT NUMBER
	5c. PROGRAM ELEMENT NUMBER

6. AUTHORS	5d. PROJECT NUMBER
Amalia E. Barrios	5e. TASK NUMBER
	5f. WORK UNIT NUMBER

7. PERFORMING ORGANIZATION NAME(S) AND ADDRESS(ES)	8. PERFORMING ORGANIZATION REPORT NUMBER
SSC Pacific 53560 Hull Street San Diego, CA 92152–5001	TR 3079

9. SPONSORING/MONITORING AGENCY NAME(S) AND ADDRESS(ES)	10. SPONSOR/MONITOR'S ACRONYM(S)
SSC Pacific Naval Innovative Science and Engineering Program 53560 Hull Street San Diego, CA 92152-5001	11. SPONSOR/MONITOR'S REPORT NUMBER(S)

12. DISTRIBUTION/AVAILABILITY STATEMENT

Approved for public release.

13. SUPPLEMENTARY NOTES

This is work of the United States Government and therefore is not copyrighted. This work may be copied and disseminated without restriction.

14. ABSTRACT

This report summarizes the methodology developed to improve the radar threshold modeling capability within the Advanced Refractive Effects Prediction System (AREPS). This work is a culmination of a joint U.S.-Netherlands (NL) project of the Coalition Warfare Program (CWP). The objective of the CWP effort is to enhance radar modeling to enable improved situational awareness of the detection capability of phased array radars, as affected by current meteorological and oceanographic (METOC) conditions.

15. SUBJECT TERMS

radar threshold modeling, advanced refractive effects prediction system, Coalition Warfare Program, detection capability, phased array radars,; meteorological and oceanographic conditions

16. SECURITY CLASSIFICATION OF:			17. LIMITATION OF ABSTRACT	18. NUMBER OF PAGES	19a. NAME OF RESPONSIBLE PERSON
a. REPORT	b. ABSTRACT	c. THIS PAGE			Amalia Barrios
U	U	U	U	31	19B. TELEPHONE NUMBER *(Include area code)* (619)553-1429

INITIAL DISTRIBUTION

Approved for public release.

SSC Pacific
San Diego, CA 92152-5001